THE EFFECT OF RELATIVE SPEED OF MOVING NOISE SOURCES ON THE MOVING FRAME ACOUSTIC HOLOGRAPHY

Soon-Hong Park, Yang-Hann Kim and Kyung-Uk Nam
Center for Noise and Vibration Control, Korea Advanced Institute of Science and Technology, Science Town, Taejon, 305-701, Korea

ABSTRACT

Moving frame acoustic holography (MFAH) enables us to visualize the noise generated by moving noise sources by using a line array of microphones affixed to the ground. The method uses the relative coordinate transformation that relates the sound pressure on the measurement and the hologram coordinate. However, the transformation is valid only when a moving line array of microphone measures the sound field of a non-moving noise source. If a line array of microphones affixed to the ground measures the sound of a moving noise source, this transformation produces errors on the hologram. This is a nontrivial drawback of MFAH. This paper studies these errors theoretically and proposes a correction method.

1. INTRODUCTION

If we attempted to use nearfield acoustic holography (NAH) [1] to analyze the noise generated by moving noise sources, we would be able to measure the pressure on a moving plane affixed to the noise sources. This requires a planar array of microphones affixed to the noise sources. Its complexity and cost limit the practical applicability of NAH to the case of moving noise sources. As a practical way of moving noise source visualization, a beamforming method [2-11] that employs a line array of microphones standing on the ground has been mostly used. The method finds the source location of noise sources, not the whole acoustic variables that NAH provides; e.g., sound pressure, particle velocity and acoustic intensity and power.

Recently proposed moving frame acoustic holography (MFAH) [12,13] can extend the practical applicability of NAH. The method uses a line array of microphones which continuously scans a sound field and produces the hologram of the scanned plane. A practical mean of implementing MFAH is to install a line array of microphones on the ground. The simplicity of the measurement system has enabled us to visualize the noise generated by moving sources based on NAH, which is the advantage of MFAH.

However, MFAH has inherent limitations due to the relative coordinate transformation, which transforms the pressure in the measurement coordinate into the hologram. The transformation is valid only when a moving line array of microphones scans the sound field of a non-moving noise source. In the case of moving noise sources, the transformation cannot correctly transform the measured pressure into the hologram. This will produce errors on the hologram and the predicted sound fields.

This paper theoretically investigates the errors of which are caused by the velocity of a noise source. The analysis eventually shows that the errors are small enough to be neglected if the speed of moving noise source is small compared with the speed of sound. It was possible by generalizing Huygens' principle [14] so that it expresses the sound field of a moving noise source as the superposition of those of distributed moving monopoles. This paper also explains the way to eliminate the errors on a hologram.

2. EFFECTS OF MOVING NOISE SOURCES ON A HOLOGRAM

Huygens' principle states that any sound field in an unbounded medium can be expressed as the superposition of elementary sound fields of distributed monopoles. It can be derived from the Kirchoff-Helmholtz integral equation [15]. This expression can be generalized for the case of moving noise sources [16], that is

$$p(\vec{X},t)=\int_{-\infty}^{\infty}\int_{V(\vec{X}_S(t_S))}\frac{\delta\left(t-t_S-\left|\vec{X}(t)-\vec{X}_S(t_S)\right|/c\right)}{\left|\vec{X}(t)-\vec{X}_S(t_S)\right|}q(\vec{X}_S(t_S),t_S)dV(\vec{X}_S(t_S))dt_S \quad , \qquad (1)$$

where $\delta(\cdot)$ denotes the delta function, t_S represents the emission time and t does the observation time. $\vec{X}$ and $\vec{X}_S$ are the position vectors in the reference coordinate $[(X,Y,Z)]$ affixed to the ground (Fig. 1). This formula essentially says that general moving noise sources can be expressed in terms of distributed moving monopoles whose strength is $q\left(\vec{X}_S,t_S\right)dV(\vec{X}_S)$. In order to examine the hologram by using MFAH, we introduce two coordinate systems in addition to the reference coordinate (Fig. 1). They describe the relative motion between a noise source and a line array of microphones. One is the measurement coordinate $[(x_m,y_m,z_m)]$, fixed to the line array of microphones. The other is the hologram coordinate $[(x_h,y_h,z_h)]$, fixed to the noise source. The two coordinates move in parallel and their relative velocity is $\vec{u}_{m/h}=\vec{u}_m-\vec{u}_h$ (Fig. 1). Note that these three coordinates coincide at $t=0$.

When a stationary line array of microphones measures the sound of a moving source, Eq. (1) can be written as

$$p^{ms}(\vec{X},t)=\int_{-\infty}^{\infty}\int_{V(\vec{X}_S(t_S))}\frac{\delta\left(t-t_S-R(t_S)/c\right)}{R(t_S)}q(\vec{X}_S(t_S),t_S)dV(\vec{X}_S(t_S))dt_S \, , \qquad (2)$$

where p^{ms} denotes the pressure due to moving noise sources and $R(t_S)=\left|\vec{X}-\vec{X}_S(t_S)\right|$.

Without loss of generality, we can reduce this equation to the case of the infinite number of distributed monopole sources. In this case, we substitute the source strength in Eq. (2) for $q(\vec{X}_S(t_S),t_S)=\sum_{n=0}^{\infty} q_n(t_S)\delta(\vec{X}_S(t_S)-\vec{X}_{S,n}(t_S))$, where q_n and $\vec{X}_{S,n}$ denote the source strength and the position vector of n-th monopole (See Fig. 2). After temporal integration, Eq. (2) can be expressed as (see reference 16 for the detailed derivation),

$$p^{ms}(\vec{X},t)=\sum_{n=0}^{\infty}\frac{q_n(t_S^*)}{\left|1-M\cos\Theta_n(t_S^*)\right|R_n(t_S^*)}, \tag{3}$$

where t_S^* has to satisfy $t-t_S^*-R(t_S^*)/c=0$ ($t_S^*<t$) and $R_n(t_S)=\left|\vec{X}-\vec{X}_{S,n}(t_S)\right|$ (See Fig. 2). M denotes a Mach number (u/c) and $\Theta_n(t_S)$ does the angle between $\vec{u}_h$ and $\vec{R}_n(t_S)$ (Fig. 2). This equation expresses the measured pressure in terms of variables associated with the emission time. It is noteworthy that the position of the noise source can be measured at the observation time. This means that Eq. (3) can be expressed in terms of variables at the observation time for the application of MFAH. If the noise source emits a sound field of frequency f_{h0} (this means $q_n(t)=q_n e^{-i2\pi f_{h0}t}$), the measured signal with respect to the observation time can be written as

$$\begin{aligned} p^{ms}(\vec{X},t)=\sum_{n=0}^{\infty}&\frac{q_n}{r_n(t)\sqrt{1-M^2\sin^2\theta_n(t)}} \\ &\times\exp\left(-i2\pi f_{h0}t+ik\frac{r_n(t)}{1-M^2}\left\{M\cos\theta_n(t)+\sqrt{1-M^2\sin^2\theta_n(t)}\right\}\right) \end{aligned}, \tag{4}$$

where $r_n(t)=\left|\vec{X}-\vec{X}_{S,n}(t)\right|$ and $\theta_n(t)$ denotes the angle between $\vec{u}_h$ and $\vec{r}_n(t)$ at the observation time (Fig. 3).

This equation represents the measured signal by a line array of microphones affixed to the ground. We denote it by $p_m^{ms}(x_m,y_m,z_m;t)$, where subscript m means the pressure in the measurement coordinate. Then we can obtain the sound field in the hologram coordinate [$p_h^{ms}(x_h,y_h,z_h;t)$] by using the relative coordinate transformation [12,13], that is,

$$x_h=u_{m/h}t+x_m,\quad y_h=y_m,\quad z_h=z_m \quad (\text{where } x_m=0 \text{ and } z_m=z_H). \tag{5}$$

Therefore, the relation between the pressure in the measurement coordinate p_m^{ms} and the pressure in the hologram coordinate p_h^{ms} can be written as [12,13]

$$p_m^{ms}(0,y_m,z_H;t)=p_h^{ms}(u_{m/h}t,y_h,z_H;t)\quad (\text{where } u_{m/h}=u_m-u_h=-u). \tag{6}$$

It is obvious that the measured pressure (p_m^{ms}) cannot correctly express a true sound field in the hologram coordinate. The obtained hologram by MFAH will have errors due to the effect of moving noise sources. From Eqs. (4) and (6), we can obtain the hologram as the complex envelope of the measured signal [13,16]

$$p_h^{ms}(u_{m/h}t, y_h, z_H; t) = \sum_{n=0}^{\infty} \frac{q_n}{r_n\sqrt{1-M^2\sin^2\theta_n}} \exp\left(ikr_n \frac{M\cos\theta_n + \sqrt{1-M^2\sin^2\theta_n}}{1-M^2} \right) \times \exp(-i2\pi f_{h0}t)$$
$$= P_h^{ms}(x_h, y_h, z_H; f_{h0}) \times \exp(-i2\pi f_{h0}t) \tag{7}$$

where $P_h^{ms}(x_h, y_h, z_H; f_{h0}) = \sum_{n=0}^{\infty} \frac{q_n}{r_n\sqrt{1-M^2\sin^2\theta_n}} \exp\left(ikr_n \frac{M\cos\theta_n + \sqrt{1-M^2\sin^2\theta_n}}{1-M^2} \right)$ is the hologram. Notice that $r_n = \left[(x_h - x_{S,n})^2 + (y_h - y_{S,n})^2 + (z_H - z_{S,n})^2\right]^{1/2}$ represents the distance between n-th noise source [$(x_{S,n}, y_{S,n}, z_{S,n})$] and a point on the hologram [(x_h, y_h, z_H), where $x_h = u_{m/h}t$]. θ_n denotes the angle between r_n and x_h axis.

Next examines the hologram that can be obtained by scanning a line array of microphone over the surface of interest. In this case, we assume that the sound source does not move, but there is the same relative motion as discussed in the previous section. We assume that a line array of microphones moves in the negative X direction with subsonic speed u. Equation (1) provides the measured pressure by the moving line array of microphones, which we denote by $p^{mm}(\vec{X}, t)$,

$$p^{mm}(\vec{X}, t) = \int_0^{t+\varepsilon} \int_{V(\vec{X}_S)} \frac{\delta(t - t_S - r(t)/c)}{r(t)} q(\vec{X}_S, t_S) dV(\vec{X}_S) dt_S, \tag{8}$$

where $r(t) = \left| \vec{X}(t) - \vec{X}_S \right|$. Notice that p^{mm} exactly express the sound pressure in the hologram coordinate by Eq. (5) (See reference 16 for details). This means we can obtain the true hologram, which we denote by $P_h^{mm}(x_h, y_h, z_H; f_{h0})$,

$$P_h^{mm}(x_h, y_h, z_H; f_{h0}) = \sum_{n=0}^{\infty} P_{h,n}^{mm}(x_h, y_h, z_H; f_{h0}), \tag{9}$$

where $P_{h,n}^{mm}(x_h, y_h, z_H; f_{h0}) = q_n \exp(ikr_n)/r_n$ for $n = 0, 1, 2, \Lambda$.

Now the effect of a general moving noise source on a hologram can be obtained from Eqs. (7) and (9),

$$P_h^{ms}(x_h, y_h, z_H; f_{h0}) = \sum_{n=0}^{\infty} \left(1 + \frac{1}{2} M^2 \sin^2\theta_n \right) e^{iMkx_h} e^{-iMkx_{S,n}} P_{h,n}^{mm}(x_h, y_h, z_H; f_{h0}). \tag{10}$$

Note that this is an approximated expression that is valid for $M << 1$ and $e^{-iMkx_{S,n}}$ is a constant [16]. This equation shows that the magnitude error is proportional to M^2. Equation (10) also states that a phase error depends on the velocity of the noise source (or, M). In other words, the phase error is proportional to M, therefore "1st order error", but the magnitude error is order of M^2, therefore 2nd order error.

3. EFFECTS ON A PREDICTED SOUND FIELD AND A METHOD OF CORRECTION

The phase error can be easily expressed in the wavenumber domain by using the 2 dimensional spatial Fourier transform. In the wavenumber domain, Eq. (10) can be written as

$$\hat{\hat{P}}_h^{ms}(k_x, k_y, z_H; f_{h0}) = \sum_{n=0}^{\infty} F_{XY}\left\{1+\frac{1}{2}M^2\sin^2\theta_n\right\} ** \hat{\hat{P}}_{h,n}^{mm}(k_x - Mk, k_y, z_H; f_{h0}) \times e^{-iMkx_{S,n}} . \quad (11)$$

Note that F_{XY} and $**$ denote the 2 dimensional spatial Fourier transform and a 2 dimensional convolution. $\hat{\hat{P}}$ denotes the wavenumber spectrum. Then, the predicted sound field can be estimated by multiplying the propagator [1] and taking the 2 dimensional inverse spatial Fourier transform, that is

$$P_h^{ms}(x_h, y_h, z_0; f_{h0}) = \sum_{n=0}^{\infty}\left(1+\frac{1}{2}M^2\sin^2\theta_n\right)\times e^{-iMkx_{S,n}} \times \int_{-\infty}^{\infty}\int_{-\infty}^{\infty}\left[\hat{\hat{P}}_{h,n}^{mm}(k_x - Mk, k_y, z_H; f_{h0})e^{ik_z(z_0-z_H)}\right]e^{i(k_x x_h + k_y y_h)}dk_x dk_y , \quad (12)$$

where z_0 denotes the z-coordinate of the prediction plane. It is noteworthy that the error tends to be zero when $M \to 0$. This equation enables us to identify the effect of the moving noise source on the predicted sound field.

The magnitude error on the prediction plane is equal to that on the hologram. We overestimate the magnitude of the predicted sound field. However, this can be neglected if M is much smaller than 1 (M<<1). The phase error gives more undesirable effect on the predicted sound field. It not only changes the initial phase of monopoles but also shifts the wavenumber spectrum [$\hat{\hat{P}}_{h,n}^{mm}(k_x - Mk, k_y, z_H; f_{h0})$]. The shifted wavenumber spectrum changes the distribution of plane waves, which consists of the sound field. Therefore, this will distort the image on the prediction plane.

However, the errors due to the shifted wavenumber spectrum can be readily corrected if the velocity of a noise source can be measured. This is possible by multiplying e^{-iMkx_h} by the obtained hologram [Eq. (10)]. This recovers the true wavenumber spectrum. Then, the corrected sound field in the prediction plane can be written as

$$P_{h,corrected}^{ms}(x_h, y_h, z_0; f_{h0}) \cong \sum_{n=0}^{\infty} e^{-iMkx_{S,n}} \int_{-\infty}^{\infty}\int_{-\infty}^{\infty}\left[\hat{\hat{P}}_{h,n}^{mm}(k_x, k_y, z_H; f_{h0})e^{ik_z(z_0-z_H)}\right]e^{i(k_x x_h + k_y y_h)}dk_x dk_y = \sum_{n=0}^{\infty} e^{-iMkx_{S,n}} P_{h,n}^{mm}(x_h, y_h, z_0; f_{h0}) ,(13)$$

where $P_{h,n}^{mm}(x_h, y_h, z_0; f_{h0})$ denotes the true sound field of each monopole on the prediction plane. This equation shows that we obtain the sum of the monopole sound fields whose initial phases are changed due to $e^{-iMkx_{S,n}}$ ($n = 0,1,2,\Lambda$). However, this can be neglected when the monopoles are distributed in a compact region

($x_{S,n} / \lambda < 1, n = 0,1,2,\Lambda$).

4. NUMERICAL EXAMPLES

The effects of moving noise sources on a hologram and a prediction plane are studied by means of a numerical simulation. We used two moving monopole sources whose initial phase is in phase with each other. The distance between them was λ. We also assumed that they move along with the positive X direction and a microphone measures the sound pressure in farfield (Fig. 4). The distance between the source and microphone is also λ (see Fig. 4). Figure 5 shows the errors according to four different velocities. The velocities are 0.05, 0.1, 0.2, and 0.3 in Mach number, respectively. Figures 5(a) and (b) show the magnitude and the phase of the hologram. These illustrate that the errors in magnitude and phase become significant as the velocity of the noise source increases. Fig. 5(c) shows wavenumber spectra on the hologram. The faster noise sources, the more wavenumber spectra shift. Figure 5(d) shows the magnitudes of predicted sound fields in the source plane. This figure demonstrates that the error in the source plane cannot be neglected for high-speed sources (M >0.1). However, Fig. 6 demonstrates that this error can be extensively reduced by using the proposed correction method. The corrected hologram is shown in Figs. 6 (a) and (b). Notice that the phase error can be compensated for [Fig. 6(b)]. This phase correction is also able to reduce the shift of wavenumber spectra [Fig. 6(c)] so that we obtain desirable results in the prediction plane [Fig. 6(d)].

6. CONCLUSIONS

The effect of moving noise sources on MFAH was investigated and a method to correct this effect was proposed. In this paper, we showed that errors on the predicted sound field are dependent on the velocity of noise sources. Numerical examples illustrate these errors and the feasibility of the correction method.

REFERENCES

[1] J. D. Maynard, E. G. Williams, and Y. Lee, "Near field acoustic holography : I. Theory of generalized holography and development of NAH," J. Acoust. Soc. Am., **78**(4), 1395-1413 (1985).
[2] B. Barsikow, W. F. King III, and E. Pfizenmaier, "Wheel/rail noise generated by a high-speed train investigated with a line array of microphones", J. Sound Vib., **118**(1), 99-122 (1987).
[3] B. Barsikow and W. F. King, III, "On removing the Doppler frequency shift from array measurements of railway noise," J. Sound Vib., **120**(1), 190-196 (1988).
[4] T. Tanaka, I. Sakamoto, T. Murakami, S. Mori, and S. Ogata, "Measurement of tyre/road noise of a running vehicle by acoustical holography," in proceedings of Inter Noise 91, (Sydney, Australia, 1991), pp.1081-1084.
[5] A. Torri, Y. Takano, K. Terada, M. Sebata, A. Iida, K. Horihata, and H. Fujita, "Shinkansens's sound source measurements using microphone arrays," in proceedings of Inter Noise 92, (Toronto, Canada, 1992) pp. 1171-1174.
[6] Y. Takano, K. Terada, E. Aizawa, A. Iida, and H. Fujita, "Development of a 2-dimensional microphone array measurement system for noise sources of fast moving vehicles," in proceedings of Inter Noise 92, (Toronto, Canada, 1992), pp.1175-1178.

[7] S. Brühl and K. -P. Schmitz, "Noise source localization on highspeed trains using different array types," in proceedings of Inter Noise 93, (Leuven, Belgium, 1993), pp. 1311-1314.

[8] J. F. Hamet, M. A. Pallas, and K. -P. Schmitz, "Deufrako-1: Microphone array techniques used to locate acoustic sources on ICE, TGV-V and TRANSRAPID 07," in proceedings of Inter Noise 94, (Yokohama, Japan, 1994), pp. 187-192.

[9] G. Hölzl, P. Fodiman, K.-P. Schmitz, M. A. Pallas and B. Barsikow, "Deufrako-2: Localized sound sources on the high-speed vehicles on ICE, TGV-V and TRANSRAPID 07," in proceedings of Inter Noise 94, (Yokohama, Japan, 1994), pp.193-198.

[10] H. Nakagawa, T. Tsuru, T. Tanaka, I. Sakamoto, "Detection and visualization of moving sound source through acoustic holography," in proceedings of ASVA 97, (Tokyo, Japan, 1997), pp.591-594.

[11] F. Poisson, J. C. Valiere and P. Herzog, "High speed sound sources localization using bilinear time-frequency transformation," Applied Acoustics, **53**, 1-13 (1998).

[12] H. -S. Kwon and Y. -H. Kim, "Moving frame technique for planar acoustic holography," J. Acoust. Soc. Am., **103**(4), 1734-1742 (1998).

[13] S. -H. Park and Y. -H. Kim, "An improved moving frame acoustic holography for coherent bandlimited noise," J. Acoust. Soc. Am, **104**(6), 3179-3189 (1998).

[14] P. M. Morse and H. Feshbach, *Methods of theoretical physics* (McGraw Hill, NewYork, 1953), Chap.7, pp. 847-848.

[15] M. E. Goldstein, *Aeroacoustics* (McGraw Hill, New York, 1976), Chap 1, pp. 32-33.

[16] S.-H. Park and Y. -H. Kim, " Effects of moving noise sources on moving frame acoustic holography (MFAH)," In preparation (1999)

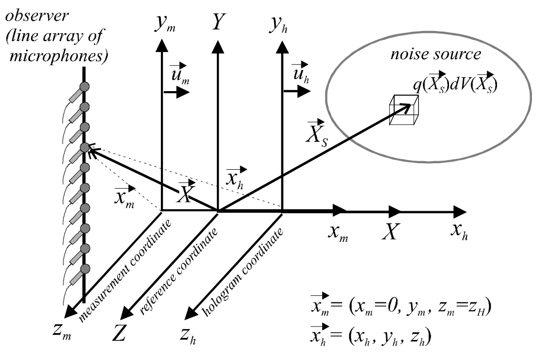

FIG. 1 Three coordinate systems

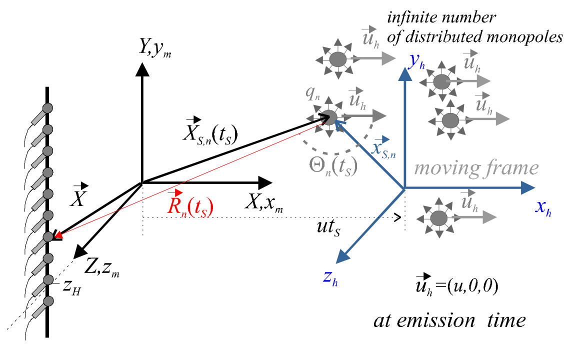

FIG. 2 Position vectors at emission time

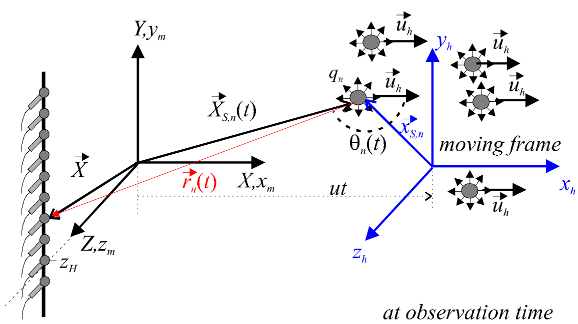

FIG. 3 Position vectors at observation time

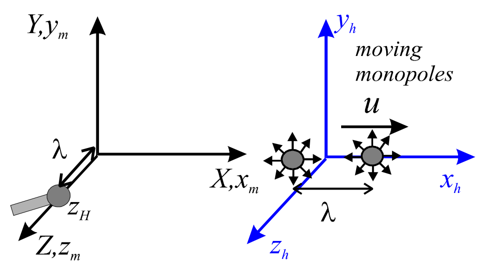

FIG. 4 Simulation configuration

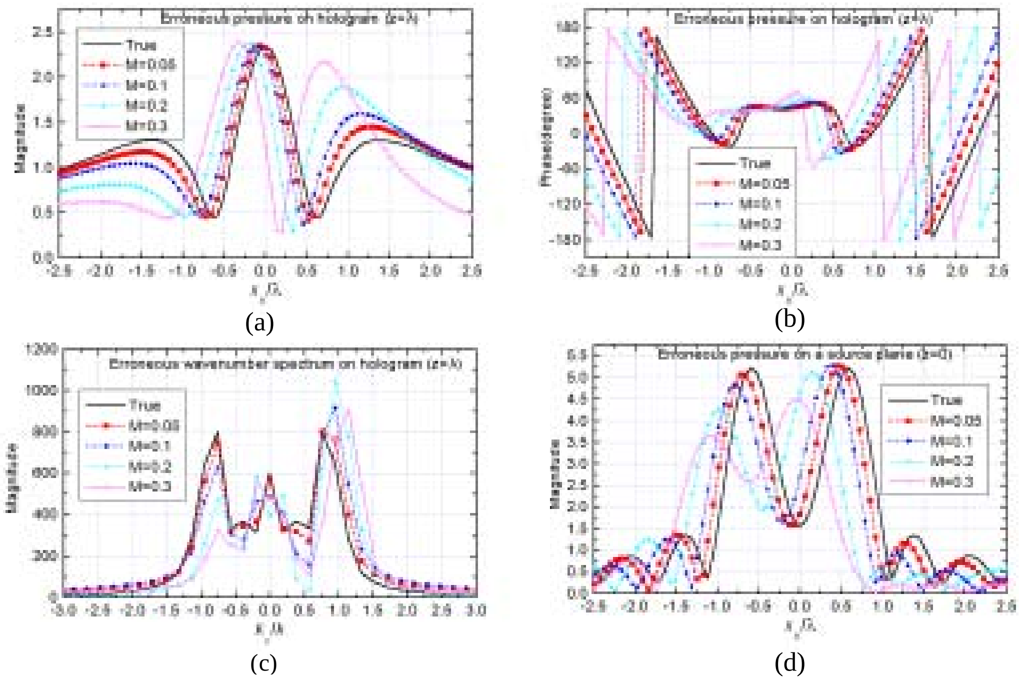

FIG. 5 Errors on hologram anda predicted sound fields according to the velocity of noise sources.

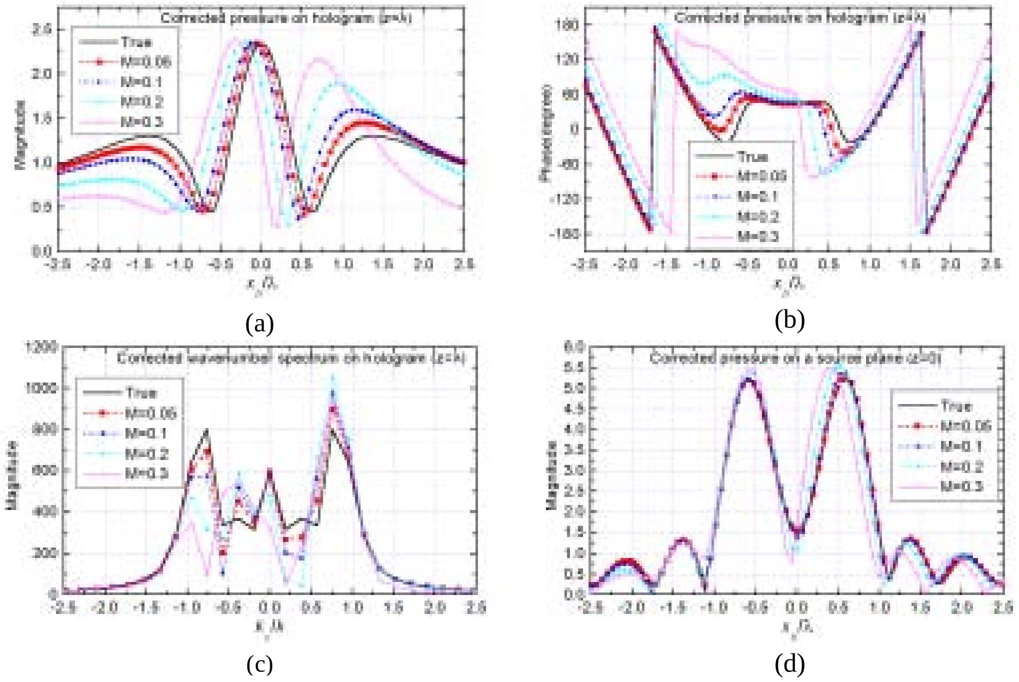

FIG. 6 The feasibility of correction method on hologram and predicted sound fields.